An improved method for extraction of mobility from space charge limited current in organic semiconductor films

S. M. H. Rizvi[a] and B. Mazhari[a]
Department of Electrical Engineering and National Centre for Flexible Electronics Indian Institute of Technology, Kanpur 208 016, India

(Received 3 February 2017; accepted 5 April 2017; published online 18 April 2017)

Estimation of mobility in thin film organic semiconductors from steady state current-voltage characteristics using Murgatroyd expression is attractive because of its simplicity but is accompanied by significant errors. These errors, resulting from neglecting diffusion current, are especially large at lower applied voltages, being more than 50% for voltages under 5 V. Using higher voltages to reduce errors is impractical in organic thin films not only due to possibility of degradation of the device but also due to distortion arising from parasitic series resistance caused by higher device currents. The present work describes an improved expression of space charge limited current for field dependent mobility that incorporates the effect of diffusion by modifying the quadratic dependence of J on voltage to $J \propto V(V + V_\beta)$, where inclusion of voltage term V_β compensates for neglecting diffusion current. Since the diffusion related voltage V_β depends on small built-in voltage that may be present under experimental conditions and, thus, is not known *a priori*, a self consistent method of extraction is described that allows extraction of V_β and mobility parameters with reduced errors up to less than 10% even for voltages under 2 V. Simulation and experimental results obtained with small-molecule Pentacene based devices are presented that illustrate the basic concept and usefulness of the proposed approach. *Published by AIP Publishing.* [http://dx.doi.org/10.1063/1.4981242]

I. INTRODUCTION

Charge carrier mobility in an organic semiconductor layer is an important transport parameter that impacts the performance of diverse range of applications, including photovoltaics, displays, lighting, analog, and digital logic circuits. Experimental methods for estimating mobility use either time dependent, frequency dependent characteristics or steady state current-voltage characteristics. Transient techniques include time-of-flight (TOF),[1] charge extraction by linearly increasing voltage (CELIV)[2] and dark injection space charge limited current (DI-SCLC).[3] TOF is a fundamental technique for mobility extraction, in which a constant external bias drifts photo-generated charge carriers present at a non-injecting contact towards the opposite contact. However, the use of TOF technique requires considerably thick samples, in the range of microns, which makes this technique difficult to apply at thin films commonly found in devices such as rectifying diodes, solar cells, organic light emitting diodes, etc. This shortcoming is overcome by CELIV and DI-SCLC techniques where an actual device is subjected to a time dependent input voltage instead of a test structure with a thick organic film. In CELIV, a linearly increasing voltage extracts equilibrium or photoinduced charge carriers, whereas in DI-SCLC, an application of voltage pulse injects charge carriers into the active layer. Current transients, thus obtained, are used to extract mobility, but its correct extraction requires constraints on RC time constant[3,4] and ramp time of the applied voltage.[4] Additionally, these techniques assume negligible diffusion current and low dispersive transport in the material,[5,6] which may cause significant errors in the extraction of mobility. Although the impact of these effects can be reduced by parameterizing relevant equations with the help of numerical model,[4,6,7] it leads to an increased complexity of the extraction of mobility in an already specialised setup.

Frequency dependent admittance/impedance measurements and steady state current-voltage ($J - V$) characteristics are the simplest non-invasive techniques which do not require any specialised set-up for the estimation of mobility. In the former method, real and imaginary parts of admittance or impedance are measured by applying a constant dc bias, superimposed on a small ac voltage, by sweeping frequency of the ac excitation. Peak frequency in susceptance (reactance), obtained from the imaginary part of admittance (impedance), is directly proportional to the carrier transit time which is utilised to calculate mobility at a particular dc bias with a suitable proportionality factor.[8–10] The relation between peak frequency and transit time is empirical and requires numerical calculations to estimate the value of proportionality constant. Its value, however, is not unique and varies for different degrees of dispersive charge transport[10] which increases the probability of error in the extraction of mobility. It is worth noting that susceptance comprises device capacitance that is also quite sensitive to shallow traps as opposed to steady-state current.[11,12]

Steady state current density-voltage ($J - V$) characteristics offer the simplest method for estimating mobility in the bulk of the semiconductor layer. Since most of the organic semiconductors are intrinsically disordered, transport of charge carriers occurs under the presence of potential barriers, resulting in an electric field dependence of mobility. This dependence is generally characterized by Poole-Frenkel

[a]Electronic addresses: rizvismh@outlook.com and baquer@iitk.ac.in, Tel.: +91 0512 2597924, Fax: +91 0512 2590063.

like mobility model $\mu = \mu_0 \exp(\gamma\sqrt{E})$, where μ_0 represents carrier mobility at zero electric field and γ is electric field (E) enhancement factor.[13] For a symmetrical device with zero built-in voltage, current voltage characteristics are approximated by an expression for space charge limited current (SCLC) proposed by Murgatroyd[14]

$$J = \frac{9}{8}\varepsilon\mu_0\frac{V^2}{d^3}\exp\left(0.891\gamma\sqrt{V/d}\right), \quad (1)$$

where J is the current density, V is the applied voltage, and ε and d are the permittivity and thickness of organic layer, respectively. Eq. (1) is also widely used to estimate charge carrier mobility in non-zero V_{bi} devices like solar cell[15–18] and organic light emitting diodes[19,20] after correction for built-in voltage and series resistance.[21] It is recognised that neglecting diffusion current is one of the key limitations of Eq. (1), and its use leads to overestimation of mobility.[12] It is also commonly implied that the errors can be reduced through a proper selection of true SCLC region in which the model would hold. However, definition of the onset of true SCLC in a $J-V$ curve lacks clarity especially in light of the recent reports that suggest diffusion current would extend well beyond few k_BT/q,[22,23] where q is the elementary charge, k_B is the Boltzmann constant and T is the temperature. In this particular work, we took an in-depth look at the errors involved in the use of Murgatroyd expression for the extraction of mobility and suggested an improved phenomenological model which allows reliable extraction of mobility even at very low voltages. The rest of this paper is organized as four sections. Section II illustrates the limitations of Murgatroyd's expression using numerical simulation results. In Section III, an improved expression for space charge limited current is proposed and mobility extraction using this model is analysed under both field independent and field dependent cases. We show in Section IV a comparison of proposed method with the conventional technique using experimental results obtained with small molecule Pentacene based device. Finally, we summarise the main conclusions of this work in Section V.

II. LIMITATIONS OF MURGATROYD'S APPROXIMATION

Equation (1) is a simplified expression based on several assumptions including current is primarily due to drift, electric field close to the injecting electrode is negligible[14] and series resistance effects can be neglected. To investigate the limitations of Murgatroyd's approximation, numerical simulations were carried out using organic device module of 2D device simulation package ATLAS.[24] It uses finite-element approach to solve drift-diffusion, Poisson's and continuity equations with Fermi-Dirac statistics. The diffusion constant is determined using generalized Einstein relation[25] and field dependent mobility value. Simulations were performed for an organic material without any background doping, energy gap of 2 eV, dielectric constant of 4, and effective density of states of $10^{22}\,\mathrm{cm}^{-3}$, and work functions of both anode and cathode were taken as 5 eV equal to the ionization potential of the organic semiconductor to ensure negligible energetic barrier at anode and cathode for Ohmic injection of holes.

For the reference device, a 100 nm thick semiconductor layer with zero field mobility $\mu_0 = 2.7\times10^{-5}\,\mathrm{cm}^2/\mathrm{Vs}$ and field enhancement factor $\gamma = 3.9\times10^{-3}\,\mathrm{cm}^{0.5}/\mathrm{V}^{0.5}$ was taken and simulations were carried out for a temperature of 300 K. Fig. 1(a) shows a typical plot of $\ln(J/V^2)$ against average electric field $\sqrt{V/d}$ that is used for obtaining mobility parameters. The Murgatroyd expression (Eq. (1)) predicts a straight line with a positive slope from which μ_0 and γ can be obtained. However, Fig. 1(a) shows that positive slope is obtained only for voltages larger than 1 V and linear behaviour is observed for voltages exceeding 3 V. If one attempts to fit straight line to the data over different voltage ranges, different values of mobility parameters are obtained, which give large errors for both μ_0 and γ, as shown in Figs. 1(b) and 1(c), respectively. The errors in estimation of zero field mobility reduce from 110% for 3–4 V range to 60% for 5–6 V range and fall below 10% only in the fitting range of 24–25 V, which is impractical for most thin film devices. As pointed earlier, application of higher bias also results in higher device current which leads to distortion of current voltage characteristics due to series resistances. Although it is possible to estimate series resistance and subtract its effect, the cancellation can never be perfect due to errors in estimation of series resistance. The impact of series resistance on errors in estimation of mobility parameters was evaluated by adding an electrode resistance of 50 Ω at the anode side and then correcting the $J-V$ data by assuming a 45 Ω resistor implying an error of 10%. The subsequent

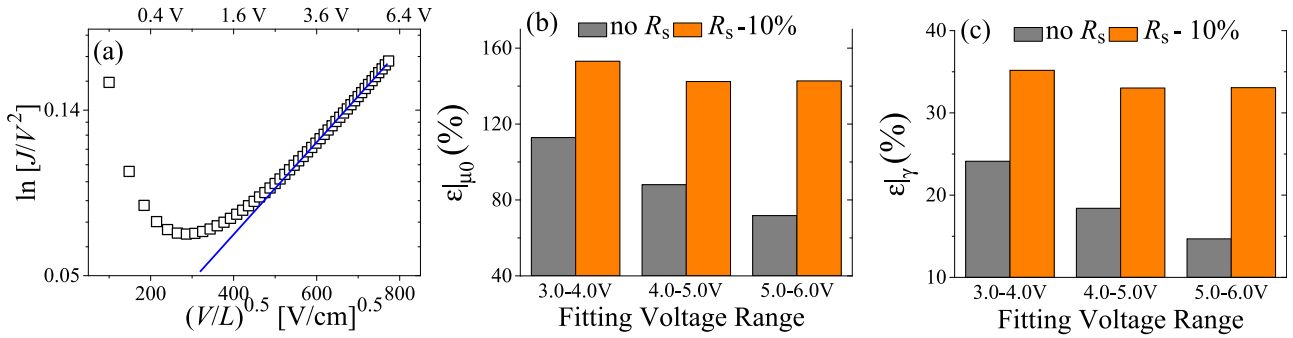

FIG. 1. (a) A plot of $\ln(J/V^2) - \sqrt{V/d}$ used for obtaining mobility parameters using Murgatroyd expression (Eq. (1)). Solid line indicates that linearity is obtained only after 3 V. Error in percentage for (b) zero field hole mobility μ_0 and (c) field enhancement factor γ at different range of fitting voltages, when there is no external resistance (grey bar) and when there is an external series resistance (orange bar) corrected with an intentional 10% error.

errors in estimation of mobility parameters are also shown in Figs. 1(b) and 1(c).

It can be seen that with series resistance present in the device, moving to higher voltage to obtain a more reliable estimate of mobility parameters is not very useful as errors become more than 100% for low field mobility and more than 30% for field enhancement factor. It can also be noted that errors stemming from series resistance are significantly larger at higher biases, thereby highlighting that for reliable estimate of mobility parameters, one needs an improved model for current that has significantly higher accuracy at lower voltages and currents.

III. AN IMPROVED METHOD FOR MOBILITY EXTRACTION

In order to reduce the errors associated with Murgatroyd's model, especially at lower voltages, we begin by addressing the limitations of Mott Gurney (MG) model for space charge limited current that forms its basis

$$J = \frac{9}{8}\varepsilon\mu\frac{V^2}{d^3}. \tag{2}$$

The main limitation of both Murgatroyd and MG model is that they neglect consideration of diffusion current. Attempts to include the effect of diffusion current analytically in the analysis of SCLC have resulted in complex solution involving either Bessel[26] or Airy functions.[27] Although numerically it is straightforward to solve drift-diffusion equations with appropriate boundary conditions at the contacts, this approach is not useful for extraction of mobility. A relatively simpler description for an ideal device with perfectly symmetrical contacts, implying zero V_{bi}, was suggested by Wetzelaer and Blom[28] where sum of Ohmic current[22] at small voltages with MG expression reproduced current for a wide range of voltages

$$J = 4\pi^2\varepsilon\mu\frac{k_BT}{q}\frac{V}{d^3} + \frac{9}{8}\varepsilon\mu\frac{V^2}{d^3}. \tag{3}$$

However, under experimental conditions, the barrier heights at the two opposite contacts, although close, are unlikely to be equal, thereby resulting in a small but non-zero built-in voltage.[29,30] A small but non-zero V_{bi} has a direct impact on equilibrium charge carrier concentration (p_0) resulting in modification of the Ohmic term in Eq. (3). In order to investigate this further, simulations were performed for zero injection barrier serving as anode and for small barrier height at the collecting contact (φ_c), referred as cathode. It can be seen in Fig. 2(a) that the presence of small barrier height at the cathode makes the hole density profile asymmetric with minima displaced from its ideal position in the middle towards cathode; second, it also causes a drop in the minimum hole concentration. Both of these reasons result in modification of the Ohmic current. Simulation results show that asymmetric profile obtained with non-zero φ_c can be considered as part of a symmetric carrier profile of an ideal zero V_{bi} device but with a larger thickness $d + d'$. The characteristic length d' increases with an increase in cathode barrier height, as illustrated in Fig. 2(b). This insight allows the expression for Ohmic current [see the Appendix] to be re-written as

$$J_{ohm} = 4\pi^2\varepsilon\mu\frac{k_BT}{q}\frac{V}{(d+d')^3}. \tag{4}$$

The presence of a small V_{bi} does not impact the second term in Eq. (3) as much because it arises primarily from injected charge, which is much larger than the charge present at equilibrium. Eq. (3) can now be re-written in a more general form as

$$J = \frac{9}{8}\varepsilon\mu\frac{V(V+V_\beta)}{d^3}, \tag{5}$$

$$V_\beta = \frac{32\pi^2k_BT}{9q\left(1+\frac{d'}{d}\right)^3}. \tag{6}$$

Equation (5) correctly predicts asymptotic behavior at both low and high voltages where diffusion related voltage V_β has a theoretical value of 0.9 V at 298 K for the ideal case of perfectly symmetrical contacts for which $d' = 0$. However, when characteristic length d' is non-zero for reasons mentioned above, the correction voltage V_β remains nearly constant at the calculated value 0.9 V for ideal case and starts decreasing afterwards as shown in Fig. 3. This decrease in correction term V_β is captured through Eq. (6), which predicts that the ratio of characteristic length to physical length will increase with barrier height, thereby reducing its magnitude that is consistent with the above explanation. It is important to note that small but non-zero V_{bi} is difficult to measure experimentally and characteristic length being dependent on effective density of states focuses on the relevance of experimental extraction for V_β.

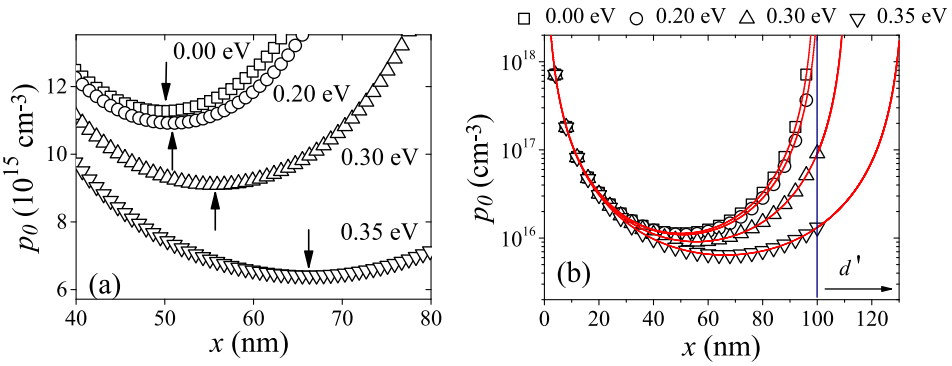

FIG. 2. (a) Equilibrium charge carrier density profile as a function of position highlighting the shift in value and position of minima for different cathode barrier heights. (b) Solid lines show fit of carrier density profiles in (a) with Eq. (A8).

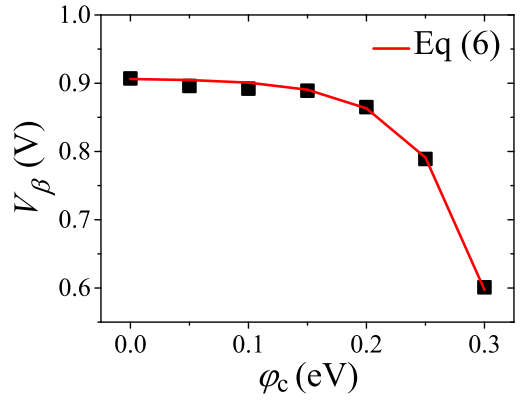

FIG. 3. Plot of extracted correction factor V_β for different barrier heights (φ_c) present at the collection electrode cathode. Solid line represents the behavior predicted by Eq. (6).

Based on the improved SCLC model, represented by Eq. (5), a modified expression for space charge limited current under Poole Frenkel mobility model can be obtained as

$$J = \frac{9}{8}\varepsilon\mu_0 \frac{V(V+V_\beta)}{d^3}\exp\left(0.891\gamma\sqrt{V/d}\right). \quad (7)$$

In order to illustrate the usefulness of Eq. (7) for extraction of mobility, we consider current-voltage characteristics of a device with a small but non-zero built-in voltage. Mobility parameters were determined using three approaches: conventional Murgatroyd expression (Eq. (1)), modified expression (Eq. (7)) with ideal value of $V_\beta = 0.9$ V and a self consistent extraction process that does not assume any *a priori* value of V_β. For the latter case, a simple iterative procedure is used to determine the value of V_β from the data itself by feeding an initial value of V_β to the function $\ln[J/(V+V_\beta)]$ and evaluating its linearity with respect to $\sqrt{V/d}$. A deviation from linear behaviour manifests itself as variation in the extracted mobility parameters for different extraction voltage ranges. The value of V_β is updated until the function becomes straight line (Fig. 4(a)) and error becomes less than 10%. As depicted in Figs. 4(b) and 4(c) when the conventional relation of Eq. (1) is used, mobility parameters show errors in excess of 100%, thus highlighting poor extraction procedure. Extraction is relatively improved when the calculated value of $V_\beta = 0.9$ V is used, but errors were still high especially in the low voltage regime which highlights the limitations of its application in practical devices. For the current example, the V_β value of 0.601 V was extracted self-consistently, as described above, to bring down the errors to less than 10%.

IV. EXPERIMENTAL RESULTS

The schematic structure of small-molecule Pentacene devices fabricated on indium tin oxide (ITO) coated glass substrates is shown in Fig. 5(a). Molybednum oxide (MoO_3) was used, as indicated by the energy level alignment in Fig. 5(b), to ensure Ohmic contacts and symmetrical current-voltage characteristic. It has been reported that deep-lying

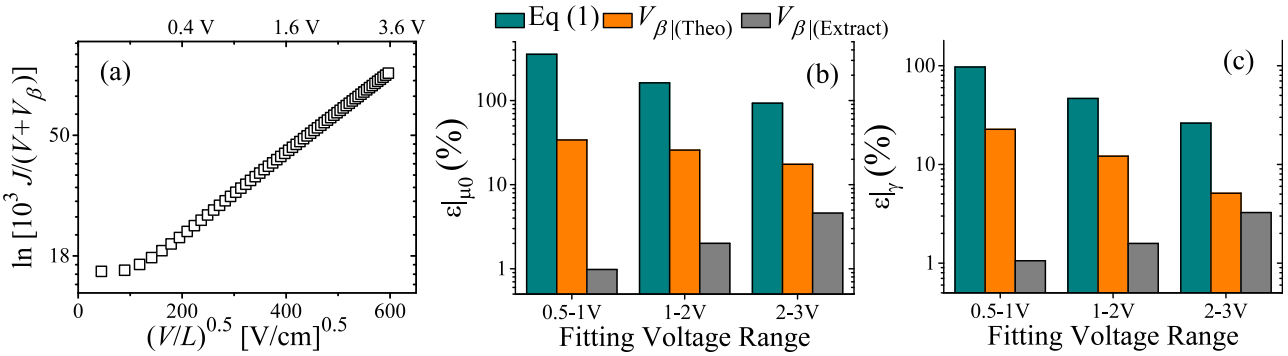

FIG. 4. (a) Plot of $\ln(J/(V+V_\beta))$ versus square root of applied field for forward (open square) where anode barrier height is zero and cathode barrier height is 0.3 eV. The corresponding error in percentage for forward characteristic for (b) zero field hole mobility μ_0 and (c) field enhancement factor γ using conventional Murgatroyd expression (Eq. (1), cyan bar), modified Murgatroyd model (Eq. (7)) when theoretical value of $V_\beta = 0.9$ V (orange bar) and self-consistent calculated value of $V_\beta = 0.601$ V (grey bar) is used, respectively.

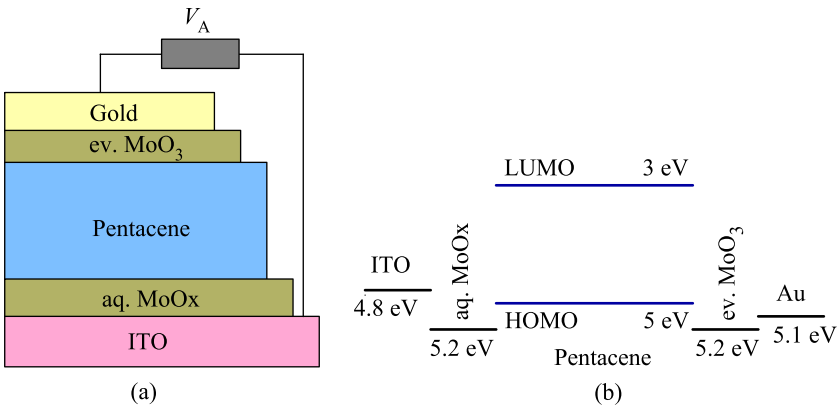

FIG. 5. (a) Zero V_{bi} device structure with a stack of ITO (150 nm), aqueous (aq.) MoOx (25 nm), Pentacene (196 nm), evaporated (ev.) MoO_3 (~10 nm) and gold (Au) (80 nm). (b) Energy level diagram of zero V_{bi} stack shown in (a) (all energy values are in eV and below vacuum level (0 eV)).

electronic states of MoO_3 facilitate good hole injection in organic semiconductors,[31] but its thickness should be small to ensure low series resistance.[32] Following patterning and cleaning of ITO substrates, 20 min of ultra-violet ozonization was carried out, followed by spin coating of a thin film (~25 nm) of aqueous molybdenum oxide[33] (aq. MoOx). Following annealing at 200 °C for 10 min on hot-plate, Pentacene was deposited at a substrate temperature of 70 °C at deposition rate of 0.3 Å/s under vacuum of 10^{-7} mbar. The thickness of the Pentacene, determined using a stylus profiler (KLA Tencor alpha-step D500), was found to be 196 nm. The deposition of Pentacene was followed by thermal evaporation (ev.) of MoO_3 powder in the same chamber at the deposition rate of 0.1 Å/s. This was followed by 80 nm thick gold (Au) as a top electrode, at deposition rate of 0.2–0.3 Å/s and at a pressure of 10^{-6} mbar to complete the device with a device area of 0.12 mm^2. Subsequently, the devices were encapsulated in nitrogen glove-box.

Steady-state $J-V$ measurements of encapsulated devices were performed using semiconductor device analyzer (Keysight B1500A) in atmospheric conditions. Application of Eq. (5) to Pentacene devices did not yield the expected linear variation implying that mobility has significant field dependence. The $J-V$ data were analyzed using Murgatroyd's expression (Eq. (1)) and corrected expression (Eq. (7)), and the results are shown in Fig. 6(a). As also observed in simulation results, compared to Murgatroyd expression, the modified expression yields linear variation over a much wider voltage range. The mobility parameters were extracted using both the techniques for two voltage ranges, and the results are shown in Fig. 6(b). It can be seen that when conventional Murgatroyd expression (Eq. (1)) is used, the extracted value of μ_0 in the low voltage range of 0.4–0.95 V is 5.75×10^{-3} cm^2/Vs and reduces to almost half to 2.92×10^{-3} cm^2/Vs for the range of 0.95–1.8 V. Similarly, for the field enhancement factor γ as well, the values 6.8×10^{-4} $cm^{0.5}\,V^{-0.5}$ and 4.2×10^{-3} $cm^{0.5}\,V^{-0.5}$ were estimated for the two voltage ranges implying an approximate variation of 84%. These large variations in estimated values over two different voltage ranges are a clear indication of lack of applicability of Murgatroyd expression to the measured data. In contrast, when the experimental data were evaluated using modified expression (Eq. (7)), mobility value in the low voltage range of 0.4–0.95 V was 7.61×10^{-4} cm^2/Vs, while for 0.95–1.8 V, the value 7.87×10^{-4} cm^2/Vs was obtained which is within approximately 3%. Similarly, a very low variation of 1.5% was calculated for γ with the values 7.78×10^{-3} $cm^{0.5}\,V^{-0.5}$ and 7.67×10^{-3} $cm^{0.5}\,V^{-0.5}$, respectively. These results were obtained with the extracted value of 0.88 V for V_β which is very close to the ideal value of 0.9 V, suggesting that device has close to zero built-in voltage. It is worth mentioning that for the upper range of 0.95–1.8 V, Murgatroyd's expression overestimates mobility by a factor of nearly 4 and underestimates field enhancement factor by approximately a factor of 2.

Besides small molecule Pentacene devices, polymer devices using P3HT (poly(3-hexylthiophene-2,5-diyl) were also fabricated and characterized. The current-voltage characteristics of ITO/aq. MoOx/P3HT (100 nm)/(ev.)MoO_3/Au showed negligible dependence of mobility on electric field, in agreement with the results reported for high molecular weight P3HT films.[34] For this case, Eq. (5) was sufficient to analyze the results and yielded a value of $V_\beta = 0.92$ V, close to the theoretical value of 0.9 V, suggesting that this might be universal for symmetrical devices with Ohmic contacts.

V. CONCLUSIONS

In summary, although steady state current-voltage characteristics of two terminal devices consisting of a single organic semiconductor layer offer the simplest method for estimating charge carrier mobility, using the commonly employed Murgatroyd expression can lead to significant errors, especially for lower applied voltages. Simulation results show that extracted value of mobility varies with the voltage range chosen for extraction and mobility can be overestimated by more than 50% for voltages under 5 V. In the present work, a correction to Murgatroyd expression is proposed to significantly reduce the errors by including the effect of diffusion current in the form of a diffusion voltage. A self-consistent method of extraction is described that allowed extraction of diffusion voltage and mobility parameters with errors reduced to less than 10% even for voltages under 2 V. This is especially important as use of low voltage minimizes the impact of series resistances due to lower device currents and also avoids degradation or damage to the device due to reduced internal electric fields. The experimental results obtained with the Pentacene devices confirmed that variation of mobility parameters with voltage range chosen for extraction is significantly reduced up to less than 3% compared to the conventional method, which yielded variations larger than 80%. The proposed modification in conventional space charge limited current with field

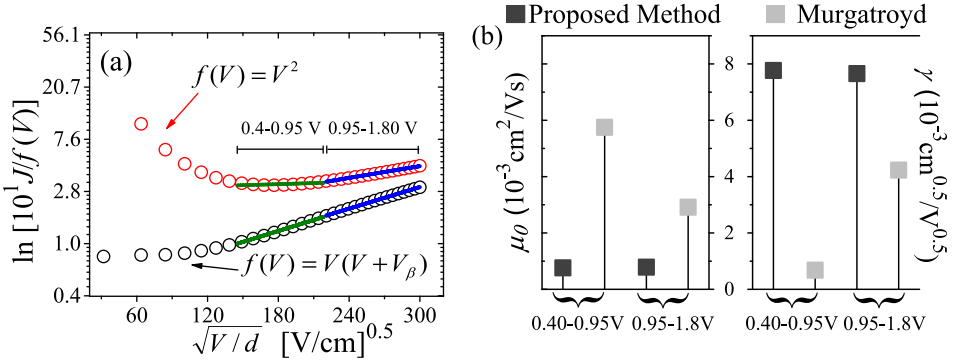

FIG. 6. (a) A representative $\ln(I/f(V))$ plot with respect to $\sqrt{V/d}$ for Pentacene devices. Green and blue solid lines show best linear fits obtained in the voltage range of 0.4 V–0.95 V and 0.95–1.8 V, respectively. (b) Extracted μ_0 (left) and γ (right) using proposed (dark square) and Murgatroyd expression (light square) at two different fitting voltage ranges at 298 K.

dependent mobility (Eq. (7)) is simple and convenient to use for interpretation of experimental results.

APPENDIX: DERIVATION OF COMPENSATION TERM V_β FOR INCORPORATING EFFECT OF DIFFUSION CURRENT IN MURGATROYD EXPRESSION

Consideration of diffusion current shows that significant charges are present in the device at equilibrium and current is zero due to a drift-diffusion cancellation process which can be written as

$$0 = qp_0(x)\mu_p E_0(x) - \mu_p k_B T \frac{dp_0}{dx}, \tag{A1}$$

where $E_0(x)$ is the electric field profile at equilibrium

$$E_0(x) = \frac{1}{p_0}\frac{k_B T}{q}\frac{dp_0(x)}{dx}. \tag{A2}$$

If we neglect any background doping, then from Gauss's law $E_0(x)$ can be related to charge density $p_0(x)$ as

$$\varepsilon \frac{dE_0}{dx} = qp_0(x). \tag{A3}$$

From (A2) and (A3), one can write

$$d(E_0)^2 = \frac{2k_B T}{q} dp_0(x), \tag{A4}$$

$$\int_{E_0(x)}^{E_0\left(x=(d+d')/2\right)} d(E_0)^2 = \frac{2k_B T}{q}\int_{p_0(x)}^{p_{m0}'} dp_0(x). \tag{A5}$$

Here, p_{m0}' is the minimum carrier concentration at equilibrium at $x = (d + d')/2$, where electric field is also zero.

$$E_0(x) = \sqrt{\frac{2k_B T}{\varepsilon}(p_0(x) - p_{m0}')}. \tag{A6}$$

From (A3) and (A6),

$$\frac{dp_0(x)}{p_0(x)\sqrt{(p_0(x) - p_{m0}')}} = \sqrt{\frac{2q^2}{k_B T \varepsilon}}dx. \tag{A7}$$

Equation (A7) is the first order differential equation with respect to x with boundary conditions $p_0|_{x=0} = N_V = p_0|_{x=d'}$ and $p_0|_{x=d} = N_V \exp(\varphi_c/k_B T)$ whose solution is given by

$$p_0(x) = \frac{2\pi^2 k_B T \varepsilon}{\left[q(d+d')\sin\left(\frac{\pi x}{(d+d')}\right)\right]^2}. \tag{A8}$$

After calculating $p_0(x)$ at equilibrium, we can further calculate the Ohmic current density by assuming quasi-equilibrium conditions at low voltages, where $p(x) \approx p_0(x)$ and mobility is assumed to be constant for low electric fields. Therefore, we can now write current density as

$$J = p_0(x)\mu_p \frac{dE_{Fp}}{dx}, \tag{A9}$$

where E_{Fp} is the quasi-Fermi level for holes in the unipolar hole only device.

$$\int_{-qV}^{0} dE_{Fp} = \int_0^d \frac{J dx}{p_0(x)\mu_p}, \tag{A10}$$

$$J_{ohm} = 4\pi^2 \varepsilon \mu \frac{k_B T}{q}\frac{V}{(d+d')^3}. \tag{A11}$$

From Eq. (3), correction term for V_β can be written as

$$V_\beta = \frac{32\pi^2 k_B T}{9q\left(1 + \frac{d'}{d}\right)^3}. \tag{A12}$$

If $d' = 0$, then it represents perfectly symmetrical contacts of a zero V_{bi} device and Eq. (A12) reduces to $32\pi^2 k_B T/9q$.

[1]T. Kreouzis, D. Poplavskyy, S. M. Tuladhar, M. Campoy-Quiles, J. Nelson, A. J. Campbell, and D. D. C. Bradley, Phys. Rev. B **73**, 235201 (2006).
[2]G. Juska, K. Arlauskas, M. V. Nas, and J. Kocka, Phys. Rev. Lett. **84**, 4946 (2000).
[3]C. H. Cheung, K. C. Kwok, S. C. Tse, and S. K. So, J. Appl. Phys. **103**, 93705 (2008).
[4]M. T. Neukom, N. A. Reinke, and B. Ruhstaller, Sol. Energy **85**, 1250 (2011).
[5]H. Li, L. Duan, D. Zhang, G. Dong, J. Qiao, L. Wang, and Y. Qiu, J. Phys. Chem. C **118**, 6052 (2014).
[6]R. Hanfland, M. A. Fischer, W. Brütting, U. Würfel, and R. C. I. Mackenzie, Appl. Phys. Lett. **103**, 63904 (2013).
[7]J. Lorrmann, B. H. Badada, O. Inganäs, V. Dyakonov, and C. Deibel, J. Appl. Phys. **108**, 113705 (2010).
[8]S. W. Tsang, S. K. So, and J. B. Xu, J. Appl. Phys. **99**, 13706 (2006).
[9]N. D. Nguyen, M. Schmeits, and H. P. Loebl, Phys. Rev. B **75**, 75307 (2007).
[10]D. C. Tripathi, A. K. Tripathi, and Y. N. Mohapatra, Appl. Phys. Lett. **98**, 33304 (2011).
[11]J. M. Montero, J. Bisquert, G. Garcia-Belmonte, E. M. Barea, and H. J. Bolink, Org. Electron. **10**, 305 (2009).
[12]E. Knapp and B. Ruhstaller, J. Appl. Phys. **112**, 24519 (2012).
[13]P. W. M. Blom and M. C. J. M. Vissenberg, Mater. Sci. Eng. **27**, 53 (2000).
[14]P. N. Murgatroyd, J. Phys. D: Appl. Phys. **3**, 308 (1970).
[15]R. A. Marsh, C. R. McNeill, A. Abrusci, A. R. Campbell, and R. H. Friend, Nano Lett. **8**, 1393 (2008).
[16]V. D. Mihailetchi, H. Xie, B. De Boer, L. J. A. Koster, and P. W. M. Blom, Adv. Funct. Mater. **16**, 699 (2006).
[17]M. Lenes, M. Morana, C. J. Brabec, and P. W. M. Blom, Adv. Funct. Mater. **19**, 1106 (2009).
[18]Z. He, C. Zhong, X. Huang, W. Y. Wong, H. Wu, L. Chen, S. Su, and Y. Cao, Adv. Mater. **23**, 4636 (2011).
[19]X. Qiao, Y. Tao, Q. Wang, D. Ma, C. Yang, L. Wang, J. Qin, and F. Wang, J. Appl. Phys. **108**, 34508 (2010).
[20]W. Y. Tan, D. Y. Gao, S. Zhong, J. Zhang, J. H. Zou, X. H. Zhu, W. Chen, J. Peng, and Y. Cao, Org. Electron. **28**, 269 (2016).
[21]J. C. Blakesley, F. A. Castro, W. Kylberg, G. F. A. Dibb, C. Arantes, R. Valaski, M. Cremona, J. S. Kim, and J. S. Kim, Org. Electron. **15**, 1263 (2014).
[22]M. Koehler and I. Biaggio, Phys. Rev. B **68**, 75205 (2003).
[23]J. Dacuña and A. Salleo, Phys. Rev. B **84**, 195209 (2011).
[24]*ATLAS User's Manual, Device Simulation Software*, 5.22.1.R (Silvaco International, Santa Clara, 2015), see https://dynamic.silvaco.com/dynamicweb/jsp/downloads/DownloadManualsAction.do?req=silen-manuals&nm=atlas.

[25]N. W. Ashcroft and N. D. Mermin, *Solid State Physics* (Holt, Rinehart and Winston, Philadelphia, 1976).
[26]B. Cvikl, J. Appl. Phys. **107**, 23710 (2010).
[27]K. Seki, J. Appl. Phys. **116**, 63716 (2014).
[28]G. A. H. Wetzelaer and P. W. M. Blom, Phys. Rev. B **89**, 241201(R) (2014).
[29]M. Grobosch and M. Knupfer, Adv. Mater. **19**, 754 (2007).
[30]P. Rusu and G. Giovannetti, J. Phys. Chem. C Lett. **113**, 9974 (2009).
[31]M. Kröger, S. Hamwi, J. Meyer, T. Riedl, W. Kowalsky, and A. Kahn, Appl. Phys. Lett. **95**, 123301 (2009).
[32]I. Hancox, P. Sullivan, K. V. Chauhan, N. Beaumont, L. A. Rochford, R. A. Hatton, and T. S. Jones, Org. Electron. **11**, 2019 (2010).
[33]J. Liu, X. Wu, S. Chen, X. Shi, J. Wang, S. Huang, X. Guo, and G. He, J. Mater. Chem. C **2**, 158 (2014).
[34]C. Goh, R. J. Kline, M. D. Mcgehee, E. N . Kadnikova, and J. M. Fréchet, Appl. Phys. Lett. **86**, 122110 (2005).